Cell Temperature and Head Effects on the Performances of a Direct Photovoltaic Pumping System Driven by an Induction Motor

A. Betka and A. Moussi *

Electrical Engineering Institute University of Oum El Bouaghi, Algeria E-mail: a_betka @ hotmail.com
* Associate researcher, Euro-Mediterranean Arid zone Research Center, CRSTRA, Algeria

Abstract – *The present paper describes the influence of the solar cell temperature variation and the geodetic head changing on the optimised performances of a stand-alone photovoltaic pumping system based on an induction motor driving a centrifugal pump, and where the MPPT circuit is omitted. These optimized performances such flow-rate, subsystem efficiencies and the daily water pumped amount are reached via the optimization of the motor efficiency for every operation point by a proper control of a natural VS PWM inverter feeding the motor. From the obtained simulation results, it has been concluded that in the case of a variable watertable (large depth), the flow-rate and the daily water amount decrease. Furthermore, the performances of the system are degraded once the temperature increases far from the reference value.*

Résumé – *Le présent papier présente l'influence de la variation de la température de la cellule ainsi que le changement de la hauteur géométrique sur les performances d'un système de pompage photovoltaïque au fil du soleil basé sur un moteur à induction entrainant une pompe centrifuge. Ces performances optimales tel que le débit et la quantité pompée sont obtenues via une commande judicieuse de l'onduleur à MLI alimentant le moteur. Les résultats obtenus montrent que les performances obtenues sont dégradées une fois la température ou la hauteur augmente, ce qui oblige à dimensionner le système en fonction de la température moyenne du site.*

Keywords: Efficiency – Photovoltaic – Pumping – Optimization.

1. INTRODUCTION

The direct conversion of light to electric energy is possible through the use of photovoltaic generators. Unfortunately, this energy conversion process is still characterised by a poor efficiency. This is due primarily to the physical structure constraints of the solar cells that constitute the photovoltaic source. The application of photovoltaic power supplies to water pumping has recently received increasing attention because of the expected cost reduction in photovoltaic solar panels. There are two basic desigh approaches for photovoltaic water pumping systems. One is to use a buckup battery with the pumping system and the other is to power the pump directly from the photovoltaic source without a battery. A number of experimental pumping schemes, which are driven by DC motors [12-15], exist. It has been observed, however, that many of these schemes suffer from maintenance problems due to commutator and brushes presence. Since the use of brushless permanent magnet motors [18] is limited to low power PV systems due to their high cost , a pumping system based an induction motor fed either by a voltage source inverter [1-9] or current source inverter [5] has been proposed as an attractive alternative where reliability and maintenance can be guaranteed. Different optimisation strategies have been proposed to improve the use efficiency of the generator such as maximum power tracking [16], motor efficiency optimization [4] and flow rate maximization [22-23]. The proposed scheme is a small scale system in which the photovoltaic array is directly coupled to an induction motor driving a monocellular centrifugal pump. This study fixes as a goal the maximization of the daily water pumped quantity obtained via the optimization of the motor efficiency since in direct photovoltaic irrigation pump system we should preferably store the maximum quantity of the drawn water into a buffer tank before starting irrigation. This optimization is achieved by a proper adjustment of two liberty degrees: the motor frequency and modulation index of the PWM voltage source inverter feeding the motor. It is in fact a variable air-gap flux functioning. In addition the influence of cell temperature variation and head changing are discussed. In the derivation of the system equations, some assumptions are made. The motor is supposed to be unsaturated. The power losses in the inverter and stray losses in the motor are also supposed negligible. Furthermore, dynamic equations are not taken into consideration since the system is assumed to run in steady state. In this paper, we will model each component of the system prior presenting the results via simulation. The main parts of the paper are organized as follows: Section 2 contains the description and modeling of the different components of the induction motor drive. In section 3, the proposed criterion of optimization is exposed , while in section 4, the results of simulation for cell temperature variation and geodetic head changing are presented .These two parameters can be regarded as disturbance entrees.

2. DESCRIPTION AND MODELING OF THE SYSTE M

The schematic diagram of the system analyzed in this paper is shown in Fig 1.

It consists of a photovoltaic array, a natural sinusoidal PWM voltage source inverter and a three-phase squirrel cage induction motor driving a centrifugal pump. The specification of different components is illustrated in appendix.

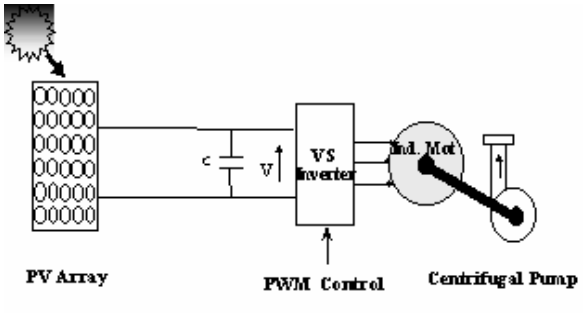

Fig.1: The PV Scheme Structure

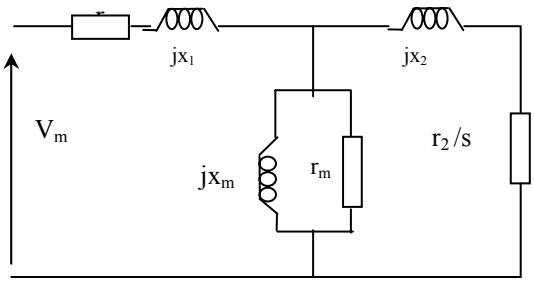

Fig .2: Per Phase Equivalent Circuit

2.1. Photovoltaic Generator Model

Photovoltaic generators are neither constant voltage sources nor current sources but can be approximated as current generators with dependant voltage sources. The array considered in this study is a 16 series connected modules type AEG.40 where the I-V characteristic can be expressed as an implicit equation:

$$I = I_{sc} - I_0 \left(\exp\left(\frac{V + R_S . I}{V_{th}} \right) - 1 \right) \tag{1}$$

The I-V curve is essentially influenced by the variation of two inputs: the solar insolation and the array temperature. The adaptation of equation (1) for different levels of solar insolation and temperature can be handled by the following equations[7]:

$$\Delta T = T - T_r \tag{2}$$

$$\Delta I = \alpha \left(\frac{E}{E_r} \right) \Delta T + \left(\frac{E}{E_r} - 1 \right) I_{sc} \tag{3}$$

$$\Delta V = - \beta \Delta T - R_s \Delta I \tag{4}$$

$$V = V_r + \Delta V \tag{5}$$

$$I = I_r + \Delta I \tag{6}$$

Where the suffix r refers to rated conditions given by E_r = 1000 W/m^2 and T_r =25^{o}C.

2.2. Inverter Model

A natural PWM switching technique is used to drive the full bridge DC-AC inverter with a modulation index M and the ratio between the frequencies of the carrier and modulating waveforms P. It is shown from [21] that for P > 9 :

- The rms value of the fundamental motor voltage V_m is given by:

$$V_m = \frac{M . V}{\sqrt{2}} \tag{7}$$

- The harmonics which appear as sidebands centred around the switching frequency multiples (k.P.f) are naturally filtered by the motor itself.

2.3. Three phase Induction Motor Model

The steady state performance of the induction motor is modelled using the conventional equivalent circuit shown in Fig. 2. The input electric power is, then, given by :

$$P_{abs} = 3 . R_{eq} . \frac{V_m^2}{Z_{eq}^2} \tag{8}$$

Where Z_{eq} is the equivalent input impedance per phase : $Z_{eq} = R_{eq} + jX_{eq}$ (9)

The mechanical equation is given by: $T_e = T_r + T_0 . \omega$ (10)

where the electromagnetic torque T_e is given by [21]:

$$T_e = 3.p.\left(\frac{V_m}{\omega_s}\right)^2 \frac{\omega_{sl} . \frac{x_m^2}{r_2}}{\left[r_1 - \frac{\omega_{sl}}{\omega_s . r_2} \left(x_{11} x_{22} - x_m^2 \right) \right]^2 + \left[x_{11} + \frac{\omega_{sl} r_1 x_{22}}{\omega_s r_2} \right]^2} \tag{11}$$

The centrifugal pump load torque T_r is assumed to be proportional to the square of the rotor speed:

$$T_r = C\left(1-\frac{\omega_{sl}}{\omega_s}\right)^2.\omega_s^2 \quad (12)$$

C is a constant which depends on pump nominal data and T_o is the friction coefficient .

2.4. Centrifugal Pump Model

The Flow-Head characteristic of a centrifugal pump can be approximated by quadratic form using Pfleider-Peterman model [23], in which the rotor speed ω is a parameter:

$$H = a_0.\omega^2 + a_1.\omega Q + a_2.Q^2 \quad (13)$$

where the motor speed ω is expressed as : $$\omega = \left(1-\frac{\omega_{sl}}{\omega_s}\right).\omega_s \quad (14)$$

a_0, a_1 a_2 are constants depending on the pump dimensions.

The pump efficiency is defined as the ratio of the hydraulic power imparted by the pump to the fluid to the shaft mechanical power and is given by :

$$\eta_p = \frac{\rho g H Q}{C\left(1-\frac{\omega_{sl}}{\omega_s}\right)^3 \omega_s^3} \quad (15)$$

The Q-H characteristic of the pipe network can be expressed by [22]: $H = H_g + \psi Q^2$ (16)

Ψ is a constant which depends on conduit diameter and on all frictional losses of the pipe network.

2.5. Insolation Model

A simplified approach was elaborated according to [8], and which will serve as a first approximate quantification of the incidental insulation. This model quantifies irradiance for a standard clear day:

$$E = E_M \sin(15(t-t_{sr}))\frac{\pi}{180} \quad (17)$$

The sunrise time is chosen as : t_{sr} = 6 h.00'. To optimize the extracted electric energy, the PV array should always be operated close to its maximum output power. This will be obtained by setting up a linear relationship between the generator voltage and frequency :[9]

$$V = C_{10} + C_{11}.\, f \quad (18)$$

If the system operates at array voltage values $V < V_{op}$ the motor speed ω presents a non-minimum phase response, and highly oscillating evolutions of ω are noticed [5]. To avoid such situation, the constant C_{10} should be greater than V_{op} for low frequencies. However, C_{11} which gives the curve slope should not be too small so as the operating point would not be far from the optimum one for high insolation values. For the present study, constants are chosen as follow:

C_{10} = 260 v (corresponding to V_{op} of the insolation level, E = 100 w/m²), and C_{11} = 0.4.

For cell temperature variation, C_{10} showed by equation (20) is fitted as a function of temperature by the following expression : $C_{10} = 219.17 - 0.8743.\, T$

Proposed Approach : In this paper, a correction of the motor efficiency by a variable air-gap flux operation is proposed and represented with the quotient V_m/f. This is reached by the optimization of a non-linear criterion representing the motor efficiency and by varying two degrees of liberty :

- The inverter frequency 'f'.
- The modulation index 'M'.

For an implementation, f indicates the frequency of the modulation waveform.

Optimisation Criterion : The maximization of the motor efficiency is chosen as the optimization criterion which makes possible determining the momentary value of the vector : $X = [\, \omega_{sl}\ f\ I\ M\,]^T$ (19)

optimizing the criterion*:* $J = \max f(X)$ (20)

where f (X) is the motor efficiency given by : $$f(X) = \frac{C.(1-\frac{\omega_{sl}}{2.pi.f})^3.(2.pi.f)^3}{(V_{th}.\ln(\frac{I_{sc}-I+I_o}{I_o})-I.R_s).I} \quad (21)$$

subject to the equality constraints : ***g (X) = 0*** (22)

In addition, the generator current I and the modulation index M are limited as follows :

$$0 \le I \le I_{sc} \quad (23)$$

$$0 \le M \le 1 \quad (24)$$

The optimisation sequences are carried out using the 'FMINCON' function of the software 'MATLAB'. After performing optimisation, the daily pumped water quantity is defined as : $D = \int_{t_{sr}}^{t_{ss}} Q dt$ (25)

3. SIMULATION AND RESULTS

The simulation is carried out on a system comprising a suction and a delivery tank, that are separated by a single pipeline. The volume of the two buffer tanks are respectively: 2.88 m^3 and 0.78 m^3, while the geodetic head of the plant is: $H_g = 7.4$ m.

Influence of Temperature Variation: As known, meteorological parameters, especially the array temperature, do not remain constant all day long, but change considerably. It is, then, worth investigating the influence of the daily average temperature variation on the predicted performances of the optimized system.

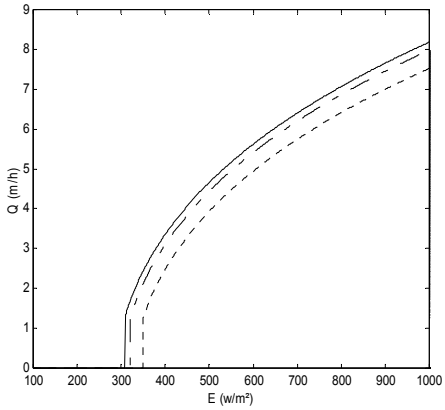

Fig. 3: Flow-rate Curves for variable Temperature

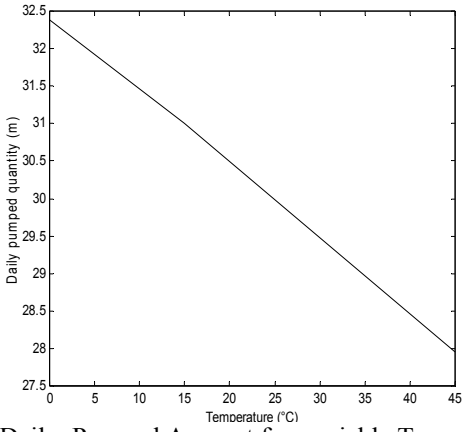

Fig. 4: Daily Pumped Amount for variable Temperature

Figures 3 through 6 display the simulation results as a function of insolation, obtained for three temperature values : T = 0°C, T = 15 °C and T = 45 °C . The geodetic head is set at : Hg = 7.4 m. As underlined in section 2, the decrease of temperature yields a significant increase of the electric power, and therefore of the motor speed. As a result, the mechanical power at the pump shaft, which varies with the cube of the motor speed, is improved. Figure 3 illustrates the flow-rate curve. This latter implies that :

- As a consequence of the speed increase, the threshold electric power (P_{eth} = 186 w) required to start pumping is obtained at a lower insolation level E_{th}, as shown in Table 1, allowing the pump to convey water earlier in the morning and ceases later at the afternoon. Doing so, we improve the solar radiation utilisability defined as the ratio of the total insolation levels that exceed the threshold value to the total available insolation over the day [9]:

$$\mu = \frac{\int_{t_1}^{t_{ss}-t_1} (E - E_{th}) dt}{\int_{t_{sr}}^{t_{ss}} E dt} \quad (26)$$

t_1 is the hourly time when the insolation crosses the threshold level.

- The increase of the mechanical power as a consequence of the temperature decrease leads to an improvement of the flowrate and, then, to an elevation of the daily water amount, as shown in Fig.4.

Fig.5 depicts the pump load torque , while in Fig.6 the optimized air-gap flux is plotted. From these two curves, one can notice that for a given value of the incident insolation, the load torque decreases when the temperature goes up. The appropriate air-gap flux to optimize the motor efficiency tends to decrease. In addition, This figure shows an important variation of the flux (2 to 4) which leads to a saturated situation of the motor.

Table 1: System performance for variable temperature

T(°C)	η_m (%)	η_p (%)	D (m^3)	Flux (V/Hz)	E_{th} ***(w/m²)***	μ (%)
0	43.65	65.69	32.38	4.03	308	91.34
15	73.63	65.29	31.00	3.81	320	90.67
45	73.59	64.28	27.96	3.36	349	88.71

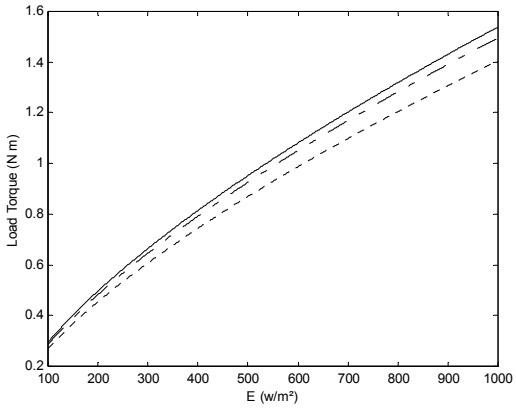

Fig. 5: Load Torque Curves

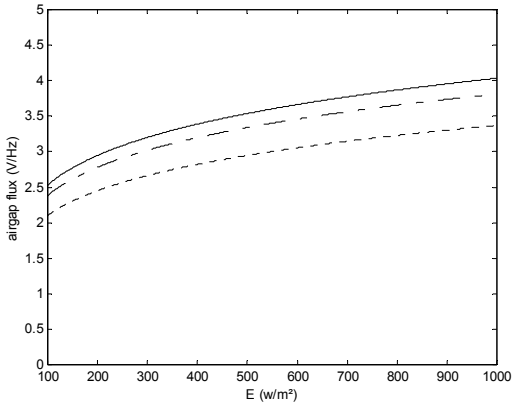

Fig. 6: Optimised Air-gap flux for variable Temperature

Influence of Head Changing: When water is discharged from a well, the inside watertable does not remain constant : It changes depending on the flowrate and the pumping time. It is, then, no longer justified to consider the geodetic head H_g as constant. Simulation runs utilizing the proposed approach where the geodetic head is changed by a step of 0.5 m. The temperature is kept constant at 25°C. The simulation results show both the threshold insolation level E_{th} and the daily water volume D as a function of the geodetic head H_g, that are respectively presented in Figure 7 and Figure 8. As can be seen, the threshold insolation and hence the electric power required to start pumping increase with head. Consequently, the daily water amount would decrease.

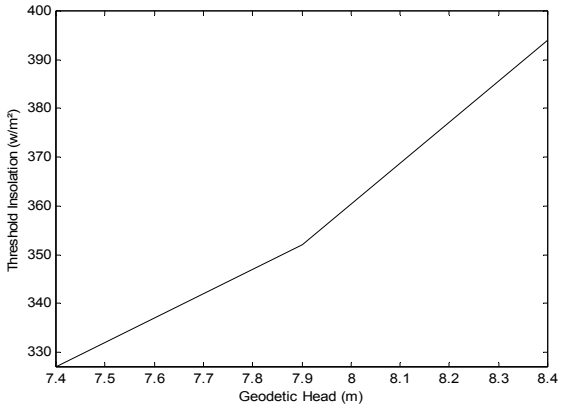

Fig. 7: Threshold Insolation Curves

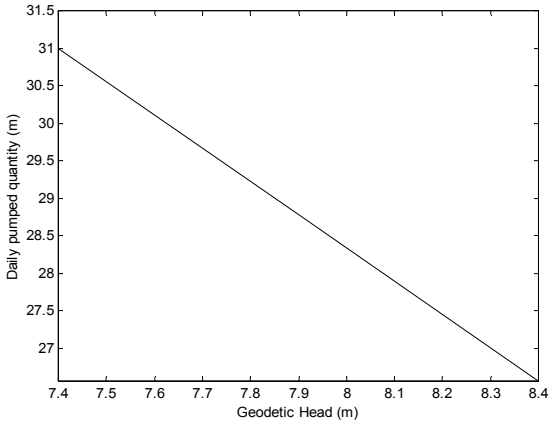

Fig. 8: Daily Pumped Quantity for Changing Head

These results confirm the behavior of a centrifugal pump which needs a relatively high speed to overcome system head. Rotating displacement pumps present a viable solution of such situation, starting pumping water at nearly zero speed, and so a least threshold electric power is required as demonstrated in [20]. In table 2, the system performances for the three considered geodetic head values and for a peak insolation level E =1000 w/m² are summarised. Since the load torque presented by equation (12) is assumed to be independent from the flow-rate, both the motor efficiency and the air-gap flux are unaffected by the head variations. In addition, the pump efficiency falls with the increase of head. This behavior is an effect of an increase of the shock losses inside the pump.

Table 2: System Performance for variable Head

H_g (m)	η_m (%)	η_p (%)	D (m^3)	Flux (V/Hz)	E_{th} (w/m²)	$P_{e\ th}$ (w)
7.4	73.6	65.4	31.00	4.02	327	186.0
7.9	73.6	64.4	28.77	4.02	352	202.3
8.4	73.6	62.7	26.57	4.02	394	283.5

4. CONCLUSION

This paper presents an optimal operation of a direct photovoltaic pumping system based on an induction motor. The optimisation criterion fixes the maximization of the motor efficiency, and where the extracted electric power is controlled by the inverter frequency instead of MPPT. The goal achieved via this study is to investigate the influence of the cell temperature and head changing effects on the system performances. The obtained simulation results show that for large depth, a decrease of both the daily pumped quantity and pump efficiency are noticed. Rotating displacement pumps present a viable solution of such situation, starting pumping

water at nearly zero speed, and so a least threshold electric power In addition, the influence of the cell temperature variation on the performance of the optimized system was also investigated. It has been concluded that these performances are degraded once the temperature increases. As a result, the sizing of the system should be done in accordance with the average daily temperature of the site.

REFERENCES

[1] S. R. Bhat, et al, ' *Performance Optimization of Induction Motor-Pump System Using Photovoltaic Energy Source*', IEEE Trans. on Ind App, Vol. 23, No. 6, 1987, pp: 995-1000.

[2] M. N. Eskandar and A. M. Zaki, ' *A Maximum Efficiency Photovoltaic-Induction Motor Pump System*', Renewable Energy, Vol. 10, No. 1, 1997, pp: 53-60

[3] R. Smith et al., ' *Analysis and Performance of Novel Two-Phase Drive for Fan and Water-Pumping Applications*', IEEE Trans on Ind App, Vol 36, No 4, November 1989, pp: 205-211

[4] B.N.Singh, et al., *' Optimized Performance of Solar Powered Variable Speed Induction Motor Drive'*, IEEE Trans. on Ind App, 1991, pp: 1201-1209.

[5] O. Olorunfemi, '*Analysis Of Current Source Induction Motor Drive Fed From Photovoltaic Energy Source'*, IEEE Trans. on Energ Conv, Vol. 6, No. 1, 1991, pp: 99-106

[6] Y. Yao, P. Bustamente and R.S. Ramshaw, ' Improvement of induction motor drive systems supplied by photovoltaic arrays with frequency control', IEEE Transactions on Energ Conv, Vol 9, No. 2, 1994, pp: 506-512

[7] D. Weiner and A. Levinson, '*water pumping optimal operation*', Electrical machines and power systems, Vol 24, No. 3, pp 277-288, 1996.

[8] K. Khousem and L. Khousem , ' *optimum matching of direct-coupled electromechanical loads to a photovoltaic generator*', IEEE Trans on Energ Conv , Vol 8, No.3, 1993, pp: 306-312

[9] R. Duzat, '*Analytic and Experimental investigation of a photovoltaic pumping system'*, PhD – work 2000, Oldenburg University Dissertation.

[10] G. B. shrertha and L. Goel, '*A Study On Optimal Sizing Of Stand Alone Photovoltaic Stations'* IEEE Trans on Energ Conv, Vol. 13, No. 4, 1998, pp: 373-377.

[11] J. Samin and al. '*Optimal sizing of Photovoltaic Systems in Varied Climates*' , Solar Energy Vol. 6, o. 2, 1997, pp: 97-107.

[12] M. M. Saied, '*Matching of DC Motor to Photovoltaic generator for Maximum Daily Gross Mechanical Energy* ', IEEE Trans on Energ Conv, Vol. 3, No. 3, 1988, pp: 465-471.

[13] J. Appelbaum, ' *Starting and Steady State Characteristics of DC Motor Powered by Solar Cell Generator* ' , IEEE Trans on Energ Conv, Vol. 1, No. 1, 1986, pp: 17-25.

[14] S. M. Alghuwainem, ' *Steady State Operation Of DC Motors Supplied From Photovoltaic Generators With Step Up Converters'*, IEEE Trans. on Energ Conv, Vol. 7, No. 2, 1992, pp: 267-271.

[15] M. Akbaba, et al., ' *Matching Of Separately Excited Dc Motors To Photovoltaic Generators For Maximum Power Output*', Solar Energy, Vol. 63, N0. 6, 1998, pp:375-385.

[16] M. Veerachary and N. Yadaiah, ' *ANN Based Peak Power Tracking For PV Supplied DC Motors'*, Solar Energy, Vol. 69, N0. 4, 2000, pp: 343-350.

[17] R. Posorsky, ' *Photovoltaic Water Pumps, An Attractive Tool For Rural Drinking Water Supply'*, Solar Energy, Vol 58 No 4-6, pp 155-163, 1996.

[18] C. L. P. Swamy et al., ' *Dynamic Performance of a permanent Magnet Brushless DC Motor Powered by a PV Array for Water Pumping'*, Solar Energy Materials and Solar Cells, Vol. 36, 1995, pp: 187-200

[19] P. Famouri and J.J. Cathey, ' *Loss Minimization Control Of An Induction Motor Drive'*, IEEE Trans. on Ind App, 1989, pp: 226-231.

[20] W. Bucher, '*Improvements in Part Load Characteristics of Deep Well Pumps- Results of Comparative Field Tests'*, 12th European Photovoltaic Solar Energy Conference, Amsterdam, April 1994.

[21] J. M. D. Murphy and F. G. Turnbull, ' *Power Electronics control of AC motors'*, Pergamon Press 1985.

[22] A. Moussi, A. Betka and B. Azoui, ' *Optimum design of a photovoltaic pumping system'*, UPEC99, Leicester UK, 1999.

[23] A.Betka and A. Moussi, 'Optimisation of photovoltaic water pump coupled with an optimal PWM invereter', 47. Internationales Kolloquium, Ilmenau University, Germany, september, 2002.

[24] R. fletcher, '*A new Approach to variable metric algorithms'*, Computer Journal, Vol.13, 1970.

APPENDIX

Subsystem	Pumps	Motor	PV Array
Specification	**Type** Centrifugal, Monocellular **Head** 14 m **Flow rate** 2.59 l/s **Speed** 3000 rpm **Power** 521 w **Pipe Network** Φ = 0.06 m H_g = 7.4 m	**Type** three-phase induction motor **Voltage** 380 v Δ **Current** 2.5 A. **Power** 1 Kw. **Speed** ***2880 rpm.*** **Resistances** r_1=22.5 Ω r_2=7.87 Ω, r_m=1.127 K Ω. **Reactances** x_1=x_2= 15.7 Ω, x_m = 586 Ω	**Type** AEG-40 polycristalline silicon **Peak power rating** 614 w @ 280 v, 2.2 A.